Prostate-Cancer-Associated I260M Variant of DNA Polymerase β Is a Sequence-Specific Mutator†

Shibani Dalal,‡ Suzanne Hile,§ Kristin A. Eckert,§ Ka-wai Sun,‡ Daniela Starcevic,‡ and Joann B. Sweasy*,‡

Department of Therapeutic Radiology and Genetics, Yale University School of Medicine, New Haven, Connecticut 06520, and Jake Gittlen Cancer Research Institute, Pennsylvania State University College of Medicine, 500 University Drive, Hershey, Pennsylvania 17033

Received June 20, 2005; Revised Manuscript Received September 21, 2005

ABSTRACT: Studies show that 30% of 189 tumors sequenced to date express variants of the polymerase β (pol β) protein that are not present in normal tissue. This raises the possibility that variants of pol β might be linked to the etiology of cancer. Here, we characterize the I260M prostate-cancer-associated variant of pol β. Ile260 is a key residue of the hydrophobic hinge that is important for the closing of the polymerase. In this study, we demonstrate that the I260M variant is a sequence context-dependent mutator polymerase. Specifically, I260M is a mutator for misalignment-mediated errors in dipyrimidine sequences. I260M is also a low-fidelity polymerase with regard to the induction of transversions within specific sequence contexts. Our results suggest that the hinge influences the geometry of the DNA within the polymerase active site that is important for accurate DNA synthesis. Importantly, characterization of the I260M variant shows that it has a functional phenotype that could be linked to the etiology or malignant progression of human cancer.

Cellular DNA sustains at least 10 000 lesions per day that are predominantly repaired by base excision repair (BER).[1] The BER machinery removes many modified bases that are generated by reactive oxygen species and alkylating agents (*1*, *2*). After the damage is recognized by a specific DNA glycosylase, it is released as a free base. Apurinic/apyrimidinic endonuclease then nicks the DNA backbone. DNA polymerase β (pol β) binds to the 3′-OH, fills the resulting gap in the DNA, and removes the deoxyribosephosphate with its deoxyribose phosphodiesterase activity.

The DNA pol β gene has been mapped to chromosome 8p, a region that is commonly deleted in different types of human cancer (*3*−*6*). Furthermore, pol β variants have been identified in colon, prostate, gastric, cervical, breast, and esophageal cancer (for a review, see ref *7*). Approximately 30% of the 189 tumors studied to date express variants of pol β that are not found in normal tissues and are not a result of common polymorphisms in the pol β gene (for examples, see refs *8*−*11*).

To determine whether the pol β tumor-associated variants have functional phenotypes that could be linked to the etiology of human cancer, we have begun to characterize their phenotypes. We have found that expression of the K289M colon- and I260M prostate-associated tumor variants in mouse cells results in cellular transformation, whereas expression of the wild type (WT) does not induce transformation in these cells (*12*). This recent study shows that cellular transformation by the tumor-associated variants has a mutational basis (*12*). Our laboratory has recently found that the K289M colon-cancer-associated pol β variant has a significantly reduced fidelity at an interrupted run of like nucleotides *in vivo* (*13*). Kinetic analysis of K289M demonstrated that it engages in misalignment-mediated misincorporation more frequently than WT pol β (*13*). We suggested that, during BER in cells, K289M induces mutations within interrupted runs of like nucleotides because of its inability to catalyze accurate DNA synthesis within these types of sequences. This could result in mutation or altered expression of a key growth control gene and lead to cancer (*13*).

The goal of the study that we describe here was to determine if the I260M polymerase variant has attributes that could result in mutations that have the potential to lead to cancer. We show that the I260M prostate-cancer-associated mutant of pol β has mutator activity within dipyrimidine sequences and induces transversions within specific sequence contexts at frequencies higher than the WT. Thus, I260M is a sequence-specific mutator. The Ile260 residue resides in the hinge of pol β that we have suggested is important for DNA polymerase fidelity (*14*−*17*). When our data are taken together with our cellular transformation studies (*12*), they strongly suggest that the I260M variant has a functional phenotype that may contribute to cancer etiology.

MATERIALS AND METHODS

Materials. Ultrapure deoxynucleoside triphosphates, ATP, and [γ-^{32}P]ATP (>6000 Ci/mmol, 150 mCi/mL) were

† This research was supported by CA16038 from the National Cancer Institute. J.B.S. is a Donaghue Investigator.

* To whom correspondence should be addressed: Department of Therapeutic Radiology, Yale University School of Medicine, 333 Cedar Street, P.O. Box 208040, New Haven, CT 06520. Telephone: (203) 737-2626. Fax: (203) 785−6309. E-mail: joann.sweasy@yale.edu.

‡ Yale University School of Medicine.

§ Pennsylvania State University College of Medicine.

[1] Abbreviations: pol β, DNA polymerase β; WT, wild-type DNA polymerase β; BER, base excision repair.

10.1021/bi051179z CCC: $30.25
Published on Web 11/10/2005

Table 1: DNA Substrate for Kinetic Assay and BER Assay[a]

substrate	sequence
45AG-U22-D22	5′-GCCTCGCAGCCGTCCAACCAAC CAACCTCGATCCAATGCCGTCC-3′ 3′-CGGAGCGTCGGCAGGTTGGTTG**A**GTTGGAGCTAGGTTACGGCAGG-5′
45CT	5′-GGCGGACTTCCGTGGCTTCTT C**T**GCCGGCGAGGGCGCAACGCCG-3′ 3′-CCGCCTGAAGGCACCGAAGAA**C**GACGGCCGCTCCCGCGTTGCGGC-5′
45AC	5′-GGCGAGGGCGCAACGCCGTAC**G** CGGTTGCTATGGCCTCGAGAGA-3′ 3′-CCGCTCCCGCGTTGCGGCATGC**A**GCCAACGATACCGGAGCTCTCT-5′
45TC	5′-GGCGAGGGCGCAACGCCGTAC**G** GGGTTGCTATGGCCTCGAGAGA-3′ 3′-CCGCTCCCGCGTTGCGGCATGC**T**CCCAACGATACCGGAGCTCTCT-5′
203T	5′-ACCGTCTATATAAACCCGCAGT**G**CGTGGGAATTTTCTGCTCCGG-3′ 3′-TGGCAGATATATTTGGGCGTCA**T**CGCACCCTTAAAAGACGAGGCC-5′
BER substrate	3′-ATGGCGCCGGCCGGCT**A**GTTCG**A**ATAACCCATG-5′ 5′-TACCGCGGCCGGCCGA**U**CAAGCTTATTGGGTAC-3′

[a] The templating base is bold and underlined.

purchased from New England Biolabs, Sigma, and Amersham Biosciences, respectively.

Construction of Mutant I260M Pol β. The mutant was generated by the Stratagene Quick-Change Site-Directed Mutagenesis kit according to the protocol of the manufacturer using pET28a-WT as a template, followed by DNA sequencing.

Protein Expression and Purification. WT and variant I260M were overexpressed in *Escherichia coli* strain BL21 (DE3) and purified as described previously (*18*).

HSV-tk Forward Mutation Spectrum. The FT334 strain with the genotype *recA13 upp tdk* was used to detect mutations in the Herpes simplex virus type 1 thymidine kinase (HSV-*tk*) gene, and the assay was carried out as described by Eckert et al. (*19*). However, the *tk* target, pSS4, carried a $[TC]_{11}$ artificial microsatellite sequence in-frame between bases 111 and 112 of the HSV-*tk* gene (*20*). The tk^- mutants are selected on 5-fluoro-2′-deoxyuridine (FUdR), which is cytotoxic in the presence of an active *tk* gene. The mutation frequency is equal to the number of tk^- colonies on FUdR divided by the total number of colonies plated, as described (*19*).

DNA Substrate Preparation for Kinetic Study and BER Assay. The DNA substrates employed in the biochemical assays described below are displayed in Table 1. The oligonucleotides used in the preparation of the DNA substrates were synthesized at the Keck Molecular Biology Center at Yale University and purified by denaturing polyacrylamide gel electrophoresis. The 5′ end of the primer was radiolabeled with [γ-^{32}P]ATP, purified by a microspin column, and annealed with template and 5′-phosphorylated downstream DNA as described (*18*).

RER Assay. This assay was carried out as described previously by Lang et al. (*13*) using the BER substrate in Table 1.

Circular Dichroism Studies. To determine if the global structure of the I260M protein was different from that of the WT, a wavelength scan (190−260 nm) of the WT and mutant pol β was carried out. The proteins were in (10 μM) in 10 mM phosphate buffer (pH 8.0) at 25 °C, and the scan was carried out in a 0.2-cm path-length quartz cuvette in a circular dichroism spectrophotometer (Aviv Model 305SF).

Presteady-State Burst Experiment. A presteady-state burst experiment was carried out as described (*18*).

Active-Site Titration. The titration was performed by preincubating a fixed concentration of pol β protein with increasing concentrations of the gapped DNA substrate (45CT or 45AC). This mixture was then reacted for 0.3 s with the correct dNTP substrate. The selected interval allowed adequate time to reach maximum amplitude with minimal contribution of multiple catalytic turnovers. This method provides a measurement of the number of active enzyme sites present and allows us to obtain the equilibrium dissociation constant, K_d, for DNA, from the equations described below.

Single-Turnover Misincorporation Assays. This experimental approach provides a way to compare the I260M variant with the WT enzyme for their relative abilities to incorporate correct and incorrect dNTPs into a primer-template by determining the equilibrium dissociation constant from the dNTP substrate, K_d, and the maximum rate of polymerization for each dNTP, k_{pol}. In the experiments reported here, we used a ratio of 2:1 (100/50 nM) active enzyme/DNA for I260M and 15:1 (750/50 nM) for WT, because the DNA-binding affinity for WT was lower than that of I260M. Under these reaction conditions, the time courses exhibited single exponentials with amplitudes approximately equal to the DNA concentration expected for single-turnover experiments. The K_d, the equilibrium dissociation constant for dNTP, and k_{pol}, the maximum rate of polymerization for correct and incorrect dNTPs for the WT and mutant, were determined under single-turnover conditions as described (*18*). All reactions were performed in 50 mM Tris-HCl at pH 8.0, containing 2 mM dithiothreitol, 20 mM NaCl, and 10% glycerol at 37 °C. All concentrations given refer to the final concentrations after mixing.

The kinetics of correct incorporation were determined using the Rapid Quench-Flow apparatus, and the concentration of dNTP ranges are 2−200 μM for WT and 5−500 μM for I260M. Misincorporation kinetics were carried out manually with dNTP concentrations ranging from 50 to 500 μM for WT and from 50−2000 μM for I260M.

Data were analyzed by Kaleidagraph software (Synergy software) with the appropriate equations as described (*18*). Data from the burst experiments were fit to the burst equation: $[\text{product}] = A(1 - \exp(-k_{obs}t) + k_{SS}t)$. Data from active-site titrations were fit to the quadratic equation: $[E-DNA] = 0.5(K_{d(DNA)} + [E]_0 + [D]_0) - [0.25(K_{d(DNA)} + [E]_0 + [D]_0)^2 - ([E]_0[D]_0)]^{0.5}$, where [E−DNA] is the concentration of the pol β−DNA complex, $[E]_0$ is the initial enzyme concentration, $[D]_0$ is the initial concentration of the gapped DNA substrate, and $K_{d(DNA)}$ is the dissociation constant of the pol β−DNA complex. To determine k_{pol} and K_d, the observed rates, k_{obs}, were plotted against dNTP

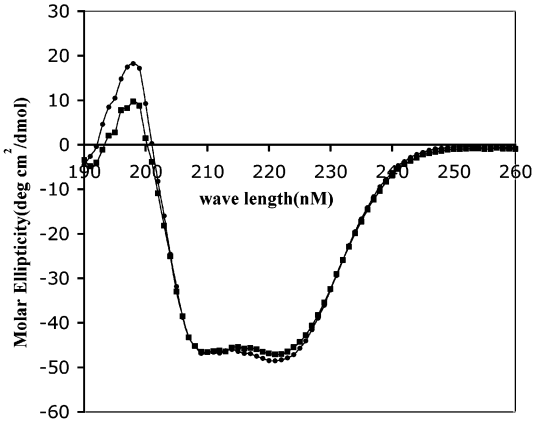

FIGURE 1: Circular dichroism for WT and mutant I260M pol β. Spectra were collected in 10 mM potassium phosphate buffer (pH 8.0) and a protein concentration of 10 μM. The spectra show that the overall folding pattern of the WT (●) and I260M (■) are similar.

concentrations and the results were fitted with the hyperbolic equation $k_{obs} = (k_{pol}[dNTP])/([dNTP] + K_d)$. Fidelity values were calculated using the relationship: fidelity $= [(k_{pol}/K_d)c + (k_{pol}/K_d)i]/[(k_{pol}/K_d)i]$, where c and i represent the correct and incorrect dNTPs, respectively.

RESULTS

I260M Exhibits Overall Folding Similar to the WT. To compare the gross structure of I260M to WT, we employed circular dichroism. The overall circular dichroism spectra of I260M and WT are similar (Figure 1A). The comparable maximal negative ellipticities at 208 and 220 nm indicated that the overall helical structure in the proteins remains intact even though residue 260 has been altered by insertion of Met in place of Ile.

I260M Exhibits Biphasic Burst Kinetics. Under conditions of excess DNA, WT shows a presteady-state "burst" of product formation with a rate of 12.0 ± 1.6 s^{-1}, as shown in Figure 2. This burst rate is similar to that obtained by us (*16*) and others (*21*). The burst is followed by a slower product release step that is rate-limiting for turnover. The same type of biphasic nature of product formation was observed in the case of I260M, as shown in Figure 2, except the burst rate is 3.4 ± 0.6 s^{-1}, which is 3.5-fold slower than that of the WT. We note that the burst amplitude of I260M appears to be lower than that of the WT, and the reason for this behavior is under investigation. These data suggest that the rate-limiting step occurs after chemistry for both WT and I260M.

I260M Induces Different Types of Mutations Than the WT. Expression of the I260M variant in mouse cells results in cellular transformation that has a mutational basis (12). Therefore, we tested the hypothesis that the I260M variant is a mutator polymerase. We characterized the frequency and types of errors induced by I260M in an unbiased approach with the HSV-*tk* forward mutation assay (19). The inaccuracy of I260M DNA synthesis through microsatellite and coding DNA sequences can be assessed using this asssay (20). In this analysis, the DNA template contained an artificial $[TC]_{11}$ microsatellite within the 5′ region of the HSV-*tk* gene; polymerase errors produced in either the repetitive or coding sequence motif will produce inactivating mutations that are detectable by the same selection scheme. The overall I260M

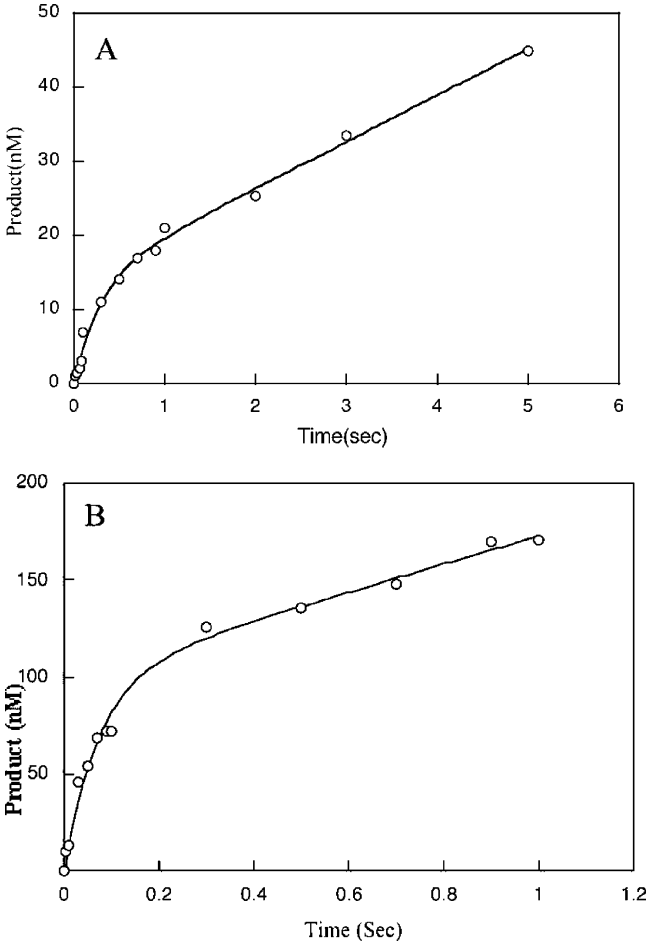

FIGURE 2: I260M exhibits biphasic burst kinetics. Insertion of dTTP into the single nucleotide gapped DNA substrate (45AG-U22-D22) was measured using the chemical quench-flow apparatus at 37 °C. A preincubated solution of 100 nM enzyme and 300 nM gapped DNA was mixed with a solution of 100 μM dTTP containing 10 mM $MgCl_2$. The reactions were quenched and monitored as described under the Materials and Methods. (A) Data for I260M were fit to the burst equation with a k_{obs} of 3.5 ± 0.6 s^{-1} and a steady-state rate constant of 1.1 s^{-1}, which is comparable to WT. (B) Data for WT were fit to the burst equation with a k_{obs} of 12.0 ± 1.6 s^{-1} and a steady-state rate constant of 1.1 s^{-1}.

polymerase error frequency with the pSS4 template was 2.3 × 10^{-2}, which is ~3-fold greater than the WT mutation frequency of 7.8 × 10^{-3}, previously reported with the pSS4 DNA substrate (20). The mutation spectrum of I260M is presented in Figure 3. Similar to the WT, the observed polymerase errors are distributed nearly equally between the microsatellite and coding-region motifs. Strikingly, approximately 90% of the canonical unit-length mutations (27/30) produced by I260M in the TC repeat are expansions of the one-repeat unit, whereas only 40% of the mutations made at this site by the WT polymerase are expansions. This difference corresponds to an 8-fold higher microsatellite expansion error frequency for I260M, relative to the WT, and the difference between polymerases in the ratio of microsatellite expansions to deletions is statistically significant ($p < 0.0003$, Fisher's exact test). In the *tk*-coding region, the I260M frameshift specificity also differs, in that 61% of the −1 base errors produced by I260M in repeated nucleotides (20/33) are at template CC and TT sequences, whereas WT only produces 27% of its errors at dipyrimidines ($p < 0.0019$). These data correspond to a 6-fold increase in the

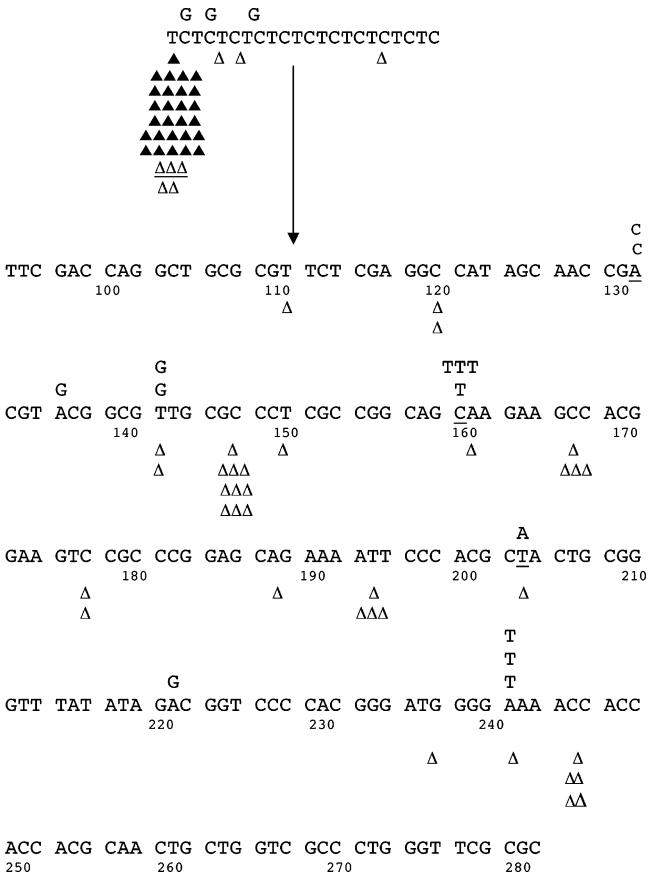

FIGURE 3: HSV-*tk* mutational spectrum of I260M. The arrow indicates the position of the $(TC)_{11}$ insertion site. One-base deletion (△), two-base deletions (△̲), and TC insertions (▲) are shown below the sequence. Base substitutions are shown above this sequence. The underlined positions shown here are sites where mutations were detected only for I260M and not WT (Eckert, unpublished data). The WT base substitutions are A to G at position 221, T to C at 142, T to C at 203, G to A at 239, C to T at 256, A to G at 242, C to T at 227, A to T at 241, and A to T at position 242.

frequency of this specific type of error produced by I260M, relative to the WT. The mutational spectrum illustrates that I260M is a mutator polymerase for misalignment errors at dipyrimidine template sequences. Polymerase error frequencies for misalignment mutations are a product of the probability of forming premutational intermediates and the efficiency of utilizing these intermediates as substrates. Previously, an exponential relationship between the WT error frequency and the number of repetitive units was observed for di- and tetranucleotide microsatellites, as well as homopolymeric coding sequences (*20*). In this study, such a relationship was not observed for I260M, a fact that we interpret as reflecting an increased efficiency of misaligned substrate utilization by I260M.

In this mutational spectrum, I260M appears to induce more transversion mutations. Of the 14 base substitution mutations induced by I260M in the *tk* target sequence itself, 57% (8/14) of them are transversions compared to 33% for the WT, a 7-fold difference in polymerase error frequency (*20*). These data indicate that I260M and WT may differ in the way that they chose the dNTP substrate for incorporation into the primer. Importantly, a comparison of the mutational spectrum of I260M to that of the WT suggests that I260M induces mutations within different types of sequence contexts than the WT. We decided to test this hypothesis by using kinetic assays.

Table 2: I260M Binds DNA More Tightly than WT

substrate	enzyme	K_d (DNA, nM)	fold over I260M
45CT	WT	48 ± 11	5
	I260M	10 ± 3	
45AC	WT	33 ± 8	8
	I260M	4 ± 0.4	

Active-Site Titration and Determination of the K_d for DNA Binding. Before we characterized the misincorporation kinetics for I260M, we measured the dissociation constant of the pol β−DNA complex, using the active-site titration assay as described in the Materials and Methods. The K_d of I260M is lower (~5−7 times) than the K_d for WT, depending upon the DNA substrates used, as presented in Table 2. This suggests that I260M binds DNA more tightly than the WT.

I260M Misincorporates dATP Opposite C. In the next series of experiments, we used the results of the HSV-*tk* assay to guide our choices of the sequence contexts of the DNA substrates that we employed in the kinetic assays. We used single-nucleotide-gapped DNA because this is most likely the DNA substrate utilized by pol β *in vivo*. Thus, the results of our kinetic assays can be used to provide insights into the functioning of the I260M variant *in vivo*.

At position 160 of the *tk* gene, we observed C to T transitions. This suggests that I260M is able to insert dATP opposite template C within this sequence context. Thus, we characterized the kinetics of misincorporation opposite template C using substrate 45CT, which has the sequence context at and surrounding position 160 of the HSV-*tk* gene. An example of our results from single-turnover experiments is presented in Figure 4. As summarized in Table 3, I260M misincorporates dATP opposite template C and shows an 8-fold decrease in fidelity compared to the WT. However, the fidelity of incorporation of dTTP or dCTP opposite C is similar for WT and I260M. The single-turnover kinetics data reveal that I260M has a very slow rate of polymerization (k_{pol}) for correct nucleotide incorporation, which results in decreased discrimination when the incorrect substrate is present in the reaction. However, I260M also exhibits less discrimination at the level of substrate binding (K_d) for misincorporation of dATP opposite C but not for dTTP or dCTP opposite C.

I260M Misincorporates Opposite Template A. Our mutation spectrum data also show that I260M produces A to C transversions at position 132. This suggests that I260M has lower fidelity than WT for misinsertion of dGTP opposite template A, within the sequence context present at position 132 of the HSV-*tk* gene. Using the 45AC DNA substrate, which has the sequence context at and surrounding position 132, we demonstrate that I260M has a 23-fold loss of fidelity, compared to the WT for insertion of G opposite template A, as shown in Table 4. To investigate the ability of I260M to induce other types of errors within this sequence context, we also assessed its ability to misinsert dATP and dCTP opposite template A. We found that I260M has a lower fidelity for insertion, compared to the WT, of dATP and dCTP opposite template A by 6- and 10-fold, respectively, as shown in Table 4. For each of these misinsertion events, we again observe that I260M has a slower rate of polym-

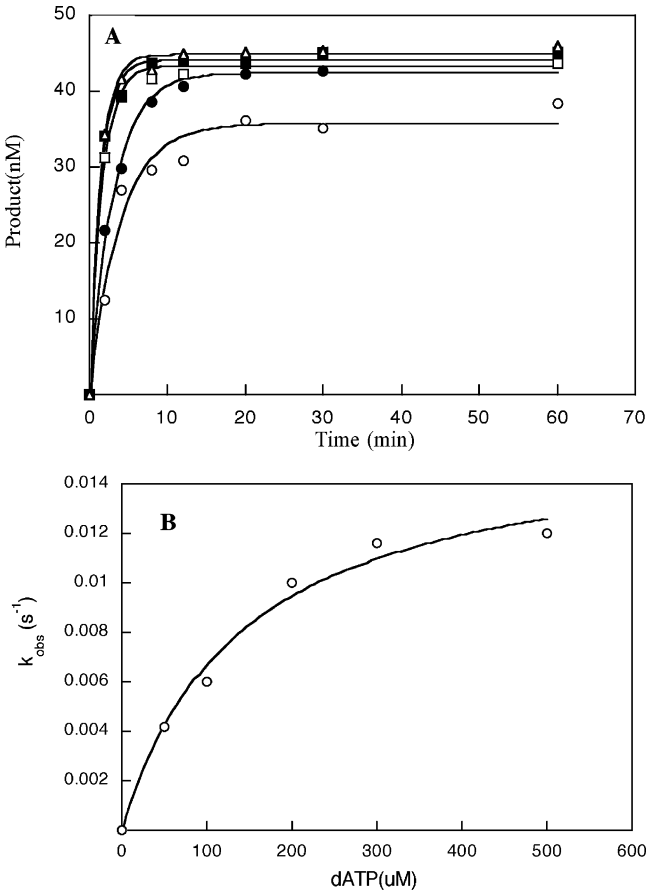

FIGURE 4: Single-turnover experiments of dATP misincorporation opposite template C. (A) Incorporation of dATP opposite template C (substrate 45CT) for I260M at 37 °C. A preincubated solution containing 100 nM enzyme and 50 nM gapped DNA substrate was mixed with 10 mM $MgCl_2$ and 50 (○), 100 (●), 200 (□), 300 (■), and 500 (△) μM dATP. The reactions were terminated by EDTA at different time points, and the product was resolved by denaturing sequencing gel electrophoresis. The data were fit to the single-exponential equation to obtain k_{obs}. (B) This figure depicts the secondary kinetic plot of k_{obs} versus the dATP concentration for I260M (○). The data were fit to a hyperbolic equation as described under the Materials and Methods. The solid line represents the best fit of the data to the hyperbolic equation. The k_{pol} is 0.015 s^{-1}, and K_d is 117.5 μM.

erization (k_{pol}) for the correct nucleotide, which results in less discrimination at the chemical step when the incorrect substrate is present. Importantly, I260M also exhibits less of an ability than WT to discriminate the correct from the incorrect substrate during the binding step for misincorporation of dGTP, dATP, and perhaps dCTP opposite template A. We note that misincorporation of dCTP opposite A could occur by slippage of the templating base, such that the G that is 5′ to the templating base serves as the templating base itself. These types of errors were most likely not observed in the *tk* assay because, in a collection of over 1000 mutants, other types of base substitutions have not been detected at position 132.

I260M Misincorporates dTTP Opposite Template T Depending upon the Sequence Context. Position 203 is the only site within the *tk* gene where we observe misincorporation by I260M of a pyrimidine opposite pyrimidine. This suggests that I260M is able to misincorporate pyrimidines opposite pyrimidines depending upon the particular sequence context. To test this hypothesis, we performed single-turnover kinetics with substrate 203T, which has the sequence context at and surrounding position 203 of the *tk* gene. We show that I260M has less fidelity than the WT opposite template T (−8-fold) (Table 5) if the incoming nucleotide is dTTP, as would be expected from the mutation spectrum. Again, it appears that I260M has a slow reaction rate (k_{pol}) for correct nucleotide incorporation, resulting in a lower fidelity for the incorporation of the incorrect nucleotide. I260M exhibits a similar level of discrimination to the WT during the binding step (K_d).

I260M Is a Polymerase That May Be Permissive for Incorporation of Purines Opposite Template A. A difference between the two DNA substrates that we used in our kinetic studies above is the nature of the templating base. In the 45AC substrate, the templating base is A, a purine. We showed that I260M misincorporates dGTP, dATP, and dCTP opposite template A (Table 4). With substrate 45CT, where the templating base, C, is a pyrimidine, it misincorporates only dATP, a purine (Table 3). However, within the 203T context, I260M has a lower fidelity for insertion of dTTP opposite template T versus the WT. This raised the possibility that I260M may be able to misincorporate purines opposite a templating purine or pyrimidine but not pyrimidines opposite a pyrimidine within certain sequence contexts. To test this hypothesis, we used kinetics to assess the effect of local sequence context on the fidelity of I260M versus the WT. We altered the templating base of our 45AC substrate from A to T. To prevent slippage-mediated misincorporation, we also changed the base 5′ to the templating base from G to C. Therefore, this new sequence context would not be found in the *tk* target. Using this new substrate (45TC), I260M has no significant difference in fidelity compared to the WT opposite template T, as we show in Table 6. Although I260M also exhibits a lower rate of polymerization (k_{pol}) with this DNA substrate, it is able to discriminate better than WT during the binding step (K_d). When our data are taken together, they suggest that alteration of Ile260 to Met results in a polymerase that has a low fidelity within certain sequence contexts.

Misincorporation Opposite Template A Is Context-Dependent. To test the hypothesis that sequence context plays an important role in DNA synthesis fidelity by I260M, we examined the fidelity of this variant with the 45AG-U22-D22 DNA substrate. This substrate has a sequence context that is not present within the HSV-*tk* gene. However, both this substrate and the 45AC substrate have a templating A and a 5′ G, but in both cases, the 3′ base and surrounding sequence are different from each other. As shown in Table 7, in 45AG-U22-D22 sequence context, I260M and WT have similar fidelities, suggesting that dGTP misincorporation opposite template A at position 132 is a sequence context-dependent event. Importantly, the maximum rate of polymerization (k_{pol}) for I260M is slower for correct nucleotide incorporation, resulting in less discrimination during chemistry when the incorrect nucleotide is present. However, this defect is compensated by the increased discrimination during the binding step (K_d) by I260M, which results in no significant loss in fidelity.

I260M Participates in BER. We constructed a uracil-containing DNA substrate and treated it with uracil DNA glycosylase (Table 1) for this assay as described (*13*). We reconstituted the *in vitro* BER assay by using whole-cell

Table 3: I260M Misincorporates dATP Opposite Template C in the *tk* Sequence Context at Position 160[a]

base pair	enzyme	k_{pol} (s^{-1})	K_d (μM)[b]	k_{polc}/k_{poli}[c]	K_{di}/K_{dc}[d]	k_{pol}/K_d (M^{-1} s^{-1})	fidelity[e] ($\times 10^3$)
C:dGTP	WT	15 ± 1	7 ± 1			21.0×10^5	
	I260M	2 ± 0.1	6 ± 1			3.3×10^5	
C:dATP	WT	0.03 ± 0.001	219 ± 20	500	31	136	16.0
	I260M	0.02 ± 0.001	118 ± 24	100	197	170	2.0
C:dTTP	WT	0.05 ± 0.007	340 ± 79	300	49	147	14.0
	I260M	0.04 ± 0.003	718 ± 139	50	120	55	6.0
C:dCTP	WT	0.02 ± 0.002	190 ± 43	750	27	105	20.0
	I260M	0.01 ± 0.0005	259 ± 20	200	43	39	8.0

[a] The correct pair is bold. [b] Units are micromolar. [c] The k_{pol} is for correct (c) divided by incorrect (i). [d] The K_d is for incorrect (i) dNTP divided by correct (c). [e] Fidelity $= [(k_{pol}/K_d)c + (k_{pol}/K_d)i]/[(k_{pol}/K_d)i]$, where c and i represent the correct and incorrect dNTPs, respectively. The DNA substrate employed is 45CT.

Table 4: I260M Misincorporates Nucleotides Opposite A in the *tk* Sequence Context at Position 132[a]

base pair	enzyme	k_{pol} (s^{-1})	K_d (μM)[b]	k_{polc}/k_{poli}[c]	K_{di}/K_{dc}[d]	k_{pol}/K_d (M^{-1} s^{-1})	fidelity[e] ($\times 10^3$)
A:dTTP	WT	18 ± 2	4 ± 0.1			45×10^5	
	I260M	4 ± 0.4	31 ± 5			1×10^5	
A:dGTP	WT	0.01 ± 0.001	310 ± 66	1800	78	32	140.0
	I260M	0.01 ± 0.0004	574 ± 99	400	19	17	6.0
A:dATP	WT	0.02 ± 0.001	103 ± 11	900	26	194	23.0
	I260M	0.01 ± 0.0001	374 ± 11	400	12	27	4.0
A:dCTP	WT	0.02 ± 0.0003	8 ± 1	900	2	2500	2.0
	I260M	0.01 ± 0.001	17 ± 5	400	1	588	0.2

[a] The correct pair is bold. [b] Units are micromolar. [c] The k_{pol} is for correct (c) divided by incorrect (i). [d] The K_d is for incorrect (i) dNTP divided by correct (c). [e] Fidelity $= [(k_{pol}/K_d)c + (k_{pol}/K_d)i]/[(k_{pol}/K_d)i]$, where c and i represent the correct and incorrect dNTPs, respectively. The DNA substrate employed is 45AC.

Table 5: I260M Misincorporates dTTP Opposite Template T in the *tk* Sequence Context at Position 203[a]

base pair	enzyme	k_{pol} (s^{-1})	K_d (μM)[b]	k_{polc}/k_{poli}[c]	K_{di}/K_{dc}[d]	k_{pol}/K_d (M^{-1} s^{-1})	fidelity[e] ($\times 10^3$)
T:dATP	WT	9 ± 1	25 ± 5			4.00×10^5	
	I260M	1 ± 0.1	56 ± 10			0.2×10^5	
T:dTTP	WT	0.01 ± 0.001	187 ± 27	643	8	53	8.0
	I260M	0.01 ± 0.00001	428 ± 1	91	8	23	1.0
T:dCTP	WT	0.02 ± 0.004	81 ± 10	530	3	247	2.0
	I260M	0.02 ± 0.003	815 ± 153	61	15	25	1.0
T:dGTP	WT	0.01 ± 0.001	4 ± 0.4	682	0.2	2500	0.1
	I260M	0.01 ± 0.001	20 ± 5	143	0.4	500	0.04

[a] The correct pair is bold. [b] Units are micromolar. [c] The k_{pol} is for correct (c) divided by incorrect (i). [d] The K_d is for incorrect (i) dNTP divided by correct (c). [e] Fidelity $= [(k_{pol}/K_d)c + (k_{pol}/K_d)i]/[(k_{pol}/K_d)i]$, where c and i represent the correct and incorrect dNTPs, respectively. The DNA substrate employed is 203T.

Table 6: WT and I260M Do Not Misincorporate a Pyrimidine Opposite Pyrimidine in 45TC Sequence Context[a]

base pair	enzyme	k_{pol} (s^{-1})	K_d (μM)[b]	k_{polc}/k_{poli}[c]	K_{di}/K_{dc}[d]	k_{pol}/K_d (M^{-1} s^{-1})	fidelity[e] ($\times 10^3$)
T:dATP	WT	9 ± 1	7 ± 1			13.0×10^5	
	I260M	1 ± 0.01	9 ± 1			1.0×10^5	
T:dTTP	WT	0.03 ± 0.001	484 ± 19	300	70	62	21.0
	I260M	0.01 ± 0.001	845 ± 200	100	93	12	8.0
T:dCTP	WT	0.03 ± 0.004	108 ± 19	300	15	277	4.0
	I260M	0.04 ± 0.003	558 ± 110	25	62	72	1.0

[a] The correct pair is bold. [b] Units are micromolar. [c] The k_{pol} is for correct (c) divided by incorrect (i). [d] The K_d is for incorrect (i) dNTP divided by correct (c). [e] Fidelity $= [(k_{pol}/K_d)c + (k_{pol}/K_d)i]/[(k_{pol}/K_d)i]$, where c and i represent the correct and incorrect dNTPs, respectively. The DNA substrate employed is 45TC.

extract (WCE) prepared from either pol β+/+ or pol β −/− mouse embryonic fibroblast cell lines. The qualitative comparison of BER performed by WT and I260M was carried out in the presence of WCE from pol β −/− cells and supplemented either with purified WT or I260M as noted in the caption of the figure. Our results show that I260M is able to participate in BER (Figure 5).

DISCUSSION

In this study, we found that the I260M prostate-cancer-associated variant has significantly lower fidelity than the WT within certain sequence contexts, as summarized in Table 8. For example, I260M has an 23-fold lower fidelity than the WT when misinserting dGTP opposite template A within the 45AC DNA substrate, but its fidelity is only 1.7-fold lower than the WT for misinsertion of dGTP opposite A within the 45AG-U22-D22 substrate. We also found that the DNA-binding affinity of I260M is higher than that of the WT. The lowered fidelity of I260M within certain sequence contexts, combined with its ability to induce cellular transformation (*12*), suggests that this tumor-associated pol β variant has a functional phenotype that is

Table 7: Misincorporation Opposite Template A Depends upon Sequence Context[a]

base pair	enzyme	k_{pol} (s^{-1})	K_d (μM)[b]	k_{polc}/k_{poli}[c]	K_{di}/K_{dc}[d]	k_{pol}/K_d (M^{-1} s^{-1})	fidelity[e] ($\times 10^3$)
A:dTTP	WT	13 ± 2	66 ± 10			2.0×10^5	
	I260M	3 ± 0.2	38 ± 70			0.7×10^5	
A:dGTP	WT	0.01 ± 0.001	314 ± 60	1300	5	32	5.0
	I260M	0.01 ± 0.0002	461 ± 47	300	12	22	3.0

[a] The correct pair is bold. [b] Units are micromolar. [c] The k_{pol} is for correct (c) divided by incorrect (i). [d] The K_d is for incorrect (i) dNTP divided by correct (c). [e] Fidelity = $[(k_{pol}/K_d)c + (k_{pol}/K_d)i]/[(k_{pol}/K_d)i]$, where c and i represent the correct and incorrect dNTPs, respectively. The DNA substrate employed is 45AG-U22-D22.

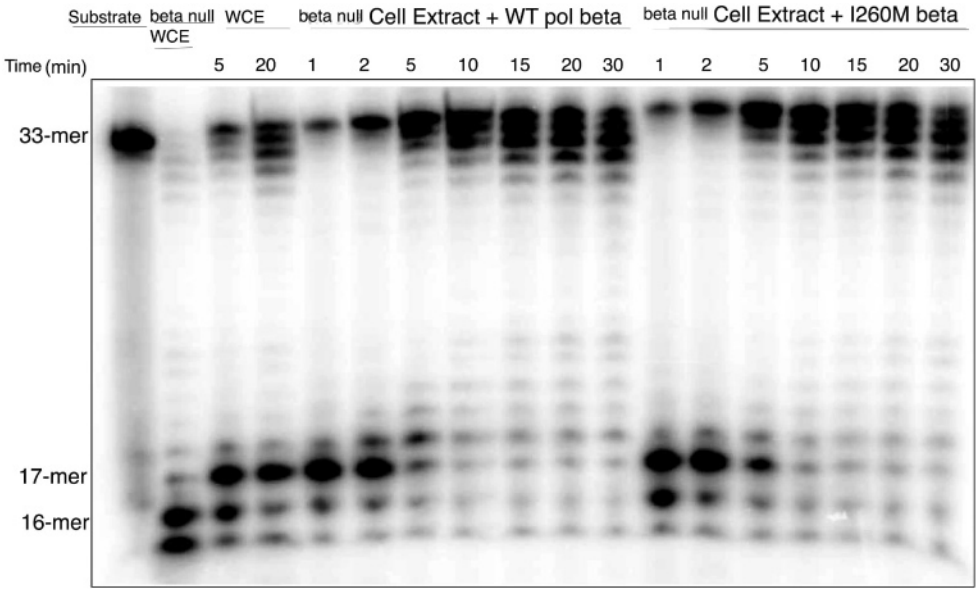

FIGURE 5: I260M participates in BER with the same efficiency as WT. Lane 1, annealed oligo substrate; lane 2, annealed oligo substrate, treated with uracil DNA glycosylase (UDG), incubated with 10 μg of pol β knockout WCE for 20 min; lanes 3−4, UDG-treated substrate, incubated with 10 μg WCE from WT cells for 5 and 20 min, respectively; lanes 5−14, UDG-treated substrate, incubated with 10 μg of pol β knockout WCE plus 2 ng of purified WT pol β for 1, 2, 5, 10, 15, 20, and 30 min, respectively; lanes 12−18, UDG-treated substrate, incubated with 10 μg of pol β knockout WCE plus 2 ng of purified I260M for the same time length as above.

Table 8: I260M Is a Sequence-Specific Mutator

template sequence[a]	DNA substrate	mispair	fidelity WT/I260M[b]
A C G	45CT	C·dA	8.0
C A G	45AC	A·dA	5.8
C A G	45AC	A·dC	10
C A G	45AC	A·dG	23
G A G	45AG-U22-D22	A·dG	1.7
A T C	203T	T·dT	8.0
C T C	45TC	T·dT	2.6

[a] The template is written 3′ → 5′, and the target base is underlined. [b] Fidelity WT/I260M is taken from Tables 3−7.

linked to the onset or progression of neoplasia. Our results also suggest that the hinge region is important for the manner in which pol β interacts with and positions DNA within its active site and that this interaction is critical for accurate DNA synthesis.

I260M Induces Different Types of Mutations Than the WT. Using the HSV-*tk* assay with the pSS4 template, we show that I260M produces a 6−8-fold higher frequency of misalignment errors at template dipyrimidine sequences and a 7-fold higher frequency of transversion errors, relative to the WT. Interestingly, I260M specifically induces expansion mutations within the $[TC]_{11}$ microsatellite. These observations suggest that alteration of hinge residue Ile260 to Met results in a polymerase that interacts with certain DNA sequence contexts in a different manner than the WT.

To characterize the mechanisms of infidelity of the I260M variant, we assessed its ability to misincorporate nucleotides within various sequence contexts, using the results of the *tk* assay to guide our thinking. Our kinetic studies show that I260M has a lower fidelity than the WT within certain sequence contexts. This suggests that I260M is not a general "sloppier copier", as are the I260Q and Y265C variant enzymes (*22*−*24*). Our results suggest that the interaction with specific DNA sequences contributes to its infidelity. Interestingly, misinsertion by the WT on undamaged templates is also influenced by sequence context (*25*).

Our results lead us to suggest that certain types of DNA sequences within prostate cells expressing I260M could be at risk for mutations induced by this variant and that a subset of these sequences would be different than those that may be at risk for mutation by the WT. Mutation of microsatellites similar to the TC repeat or dipyrimidine motifs, which tend to be located within regulatory regions of genes such as promoters and introns, could result in altered expression of key growth control genes and lead to cancer. In the case of I260M, BER may be an initiating event that creates a free primer-terminus that can misalign with complementary template residues upstream of the primer, thereby producing longer gaps where expansion may occur. I260M could also induce mutations within growth control genes that are more prone to mutation by this enzyme because of their sequence context, resulting in cancer or a more aggressive disease.

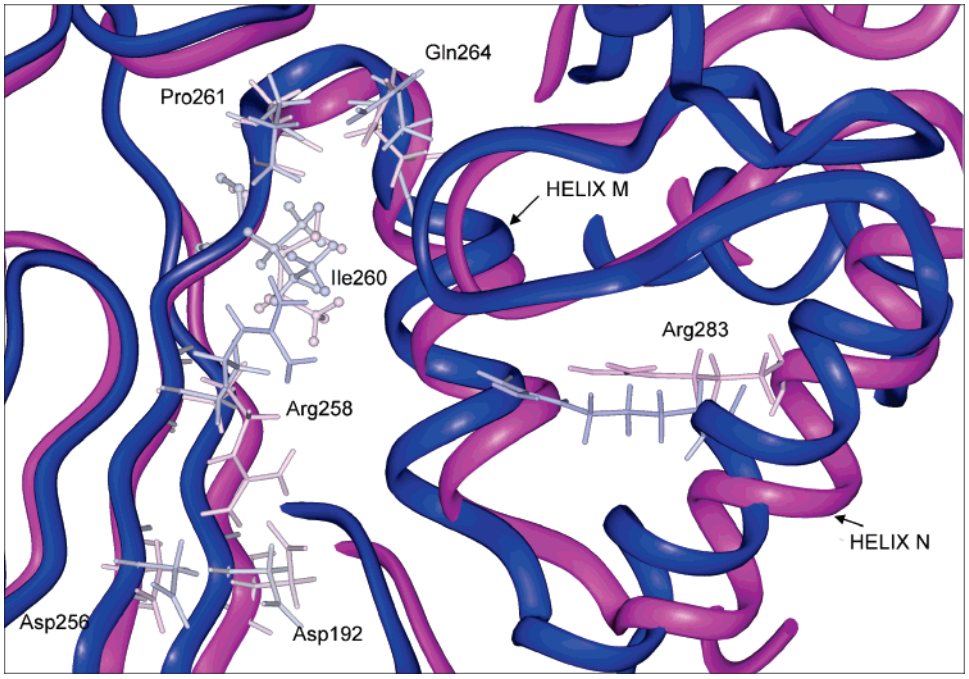

FIGURE 6: Neighboring residues of Ile260 are important for catalysis. A ribbon representation was shown for the superimposed open (pink) and closed (blue) form of pol β. α-Helix M and N are shown in arrows. The figure includes two catalytic Asp residues 256 and 192. Also shown is Arg283, which plays important role in the minor groove interaction. Hinge residue Ile260 is shown in the ball-and-stick representation. Neighboring Arg258 is presented in the stick. Recent evidence suggests that rotation of Arg258 plays an important role on pol β fidelity.

I260M Synthesizes DNA with a Lower Rate than WT Pol β. The I260M variant has a lower rate of polymerization for the correct nucleotide with each of the DNA substrates that we examined. This results in less discrimination at the level of k_{pol} when the incorrect nucleotide is present in the reaction. This suggests that alteration of the hinge of pol β influences the reaction rate.

The hydrophobic hinge consists of Leu194, Ile260, and Phe272 lining the inside and Ile174, Thr196, and Tyr265 on the outside of the hinge. The fingers domain (*26*, *27*) moves by as much as 12 Å (*28*) upon dNTP binding, and this movement originates within the hydrophobic hinge. This movement is largely due to the flexible character of the hinge loop connecting the palm and finger domains. Structural data suggest that the movement of the fingers results in alignment of the active-site residues, including Asp190, Asp192, Asp256, the 3′-OH of the primer, and the α phosphate of incoming dNTP (*28*). This geometric alignment favors rapid catalysis. Thus, alteration of the hinge by mutation could result in less stability in the closed position or aberrant closure and lead to a low reaction rate.

The overall hydrophobic nature of the hinge is maintained when Ile260 is altered to Met. Molecular modeling of energy-minimized structures suggests that there is a small change in position of each of the hinge residues in the I260M polymerase compared to the WT (data not shown). We propose that the presence of Met260 slightly alters the positioning of its neighboring residue, Pro261, as depicted in Figure 6. When pol β assumes a closed conformation, Pro261 forms a hydrogen bond with the backbone of Gln264, which is a pivotal residue in the loop that connects the palm and fingers subdomains. The hydrogen bond between Pro261 and Gln264 stabilizes the closed form of the polymerase, most likely resulting in an active site that is poised for insertion of the correct dNTP. However, slight disruption of the bond between Pro261 and Gln264 in the I260M enzyme could result in destabilization of the closed form of the polymerase, ultimately leading to a low reaction rate.

A less stable hinge could also lead to inefficient disruption of the salt bridge between Asp192 and Arg258. Because Asp192 is a key catalytic residue of pol β, retention of any interaction between residues 192 and 258 could lead to a lower rate of polymerization for correct nucleotides, which is what we observe with I260M. The Glu295 and Tyr296 residues interact with Arg258 in the closed form of pol β to diminish the interaction of Arg258 with Asp192. The salt bridge between Glu295 and Arg258 occurs along the inside of the hinge, and we predict that this interaction would also be somewhat diminished in the I260M hinge, ultimately leading to a reduced rate of polymerization.

Interestingly, a recent study of R258A and R258K mutants indicates that alteration of Arg258 to Ala would introduce additional space into the active site. Lysine, however, at the same position (258), would be predicted to decrease flexibility and delay the side-chain flipping of Arg258 (*29*, *30*). Overall, these studies suggest that Arg258 side-chain rotation plays a significant role on limiting or destabilizing the closing of pol β before chemistry (Figure 6). They also suggest that this local rearrangement will help to discourage incorrect nucleotide insertion in the active site of pol β and play a role in polymerase selectivity. We suggest that the local rearrangements that occur in the I260M active site result in a slightly reduced rate of polymerization that has little effect on fidelity with most DNA substrates. However, the slowed rotations of key residues of the enzyme in combination with certain DNA substrate structures leads to misinsertion of nucleotides or utilization of misaligned primer templates.

Infidelity of I260M Is Influenced by K_d *at Sites of Mutation.* In each of the kinetic assays that we performed, the I260M

variant had a lower polymerization rate than the WT. Importantly, in all but one case in which we observed a low fidelity of I260M versus the WT, I260M exhibited less discrimination during the binding step. In contrast, I260M did not compensate for the low rate of correct nucleotide insertion by increasing discrimination during the binding step when employing DNA substrates in which its fidelity was similar to the WT. Therefore, alteration of Ile260 to Met influences substrate discrimination during dNTP binding. Because the hinge is critical for movement of the fingers domain that contains amino acid residues that stabilize the templating base and incoming substrate, a destabilized hinge may disrupt precise positioning of these residues, resulting in a loss of discrimination during dNTP binding.

DNA Positioning Impacts upon Pol β Fidelity. It is known that rotation about the hinge positions key enzyme residues including Arg283, which appears to stabilize the templating base in position for correct dNTP insertion. We suggest that a less stable hinge could result in slightly aberrant positioning of Arg283, which, in most cases, has little effect. However, when the position of Arg283 is slightly altered in the presence of certain DNA structures, such as the one at position 132 of the *tk* gene, the geometry of the templating base is destabilized, resulting in misinsertion by I260M. Similarly, the production of expansion mutations within the [TC] microsatellite requires slippage of the nascent polypurine strand, which is expected to produce an intrahelical bulge (*20*). The altered active-site geometry of I260M may result in more favorable positioning of such bulged primer-templates for continued DNA synthesis.

Substrate choice by DNA polymerases varies depending upon the identity of the templating base, incoming dNTP, and the interaction with the neighboring protein residues. In the active site of pol *β*, the nascent base pair is sandwiched between the DNA substrate and α-helix N (*31*). Crystal structures of pol *β* show that it induces a 90° bend in the DNA upon binding, which is suggested to play an important role in polymerase fidelity (*28*). This bend is observed in the binary and ternary complexes of pol *β*. The templating base is centrally positioned within the 90° bend and is stabilized by Arg283, a residue that is present on helix N of pol *β* (*28*). Alteration of Arg283 results in a polymerase with significantly reduced activity and fidelity (*10*), suggesting that template stabilization is important for catalysis. Studies of the T79S pol *β* mutant in our lab suggest that the helix−hairpin−helix motifs adjacent to Thr79 play important roles in stabilizing the 90° bend for proper template presentation (*32*). A lack of stabilization of the DNA in this bent form results in a lowering of fidelity, as observed with the T79S mutant (*32*). Other examples that demonstrate the crucial role that template positioning plays on pol *β* fidelity include the study of the K280G variant of pol *β* (*25*, *33*) and D246V (*18*). Thus, the positioning of the DNA within the active site of pol *β* and, most importantly, the templating base plays an important role in substrate discrimination by this enzyme. We suggest that the sequence context of the DNA directly influences its ability to form or stabilize the 90° bend within the pol *β* active site that is important for the presentation of the templating base. Different sequences of DNA are predicted to assume conformations within the active site that have subtle differences from each other but that significantly impact the fidelity of the polymerase. Our study suggests that the geometries assumed by certain DNA sequences within the active site of I260M differ from their conformations in the WT. In I260M, this results in aberrant positioning or stabilization of the templating base or primer-template misalignment and ultimately leads to errors. Therefore, both the DNA conformation itself and the polymerase play critical roles in DNA fidelity.

Summary and Implications. We have shown that the prostate-cancer-associated I260M variant has a mutator phenotype specific for certain DNA sequence contexts. The mechanistic basis for misinsertion most likely resides in subtle changes in the active-site geometry of the closed conformation of pol *β* that emanates from slight alterations of the hydrophobic hinge in combination with certain DNA structures. Our data suggest that alteration of I260 to Met leads to a change in the genomic sequences that are at risk for mutation in the human genome. Prostate cancer is thought to result from complex gene−environment interactions (*34*). Although family history has been established as a risk factor for prostate cancer, only 5−10% of cases are believed to arise from major susceptibility genes. Therefore, it has been suggested that common genetic polymorphisms in combination with the environment are linked to the etiology of human prostate cancer (*34*). Pol *β* functions in the gap-filling step of BER, which is thought to be critical for the repair of at least 10 000 lesions per cell per day that result from the inherently unstable nature of DNA and from environmental insults. Much of the time, gap filling by pol *β* during BER is accurate. However, we speculate that the presence of I260M in tumor cells leads to inaccurate gap filling within certain sequence contexts, increasing the chances that certain at-risk sequences will be mutated. Thus, at-risk sequences that are present within key growth control genes in cells expressing the I260M variant could be mutated, resulting in a tumor or more aggressive disease.

ACKNOWLEDGMENT

This work was supported by PO1-CA16038 (J. B. S., project leader). We thank members of the Sweasy lab, Dr. Joachim Jaeger, and Dr. Daniel DiMaio for many insightful discussions.

REFERENCES

1. Horton, J. K., Baker, A., Berg, B. J., Sobol, R. W., and Wilson, S. H. (2002) Involvement of DNA polymerase *β* in protection against the cytotoxicity of oxidative DNA damage, *DNA Repair 1*, 317−333.
2. Lindahl, T. (2000) Suppression of spontaneous mutagenesis in human cells by DNA base excision-repair, *Mutat. Res. 462*, 129−135.
3. Eydmann, M. E., and Knowles, M. A. (1997) Mutation analysis of 8p genes POLB and PPP2CB in bladder cancer, *Cancer Genet. Cytogenet. 93*, 167−171.
4. MacGrogan, D., Levy, A., Bostwick, D., Wagner, M., Wells, D., and Bookstein, R. (1994) Loss of chromosome arm 8p loci in prostate cancer: Mapping by quantitative allelic imbalance, *Genes, Chromosomes Cancer 10*, 151−159.
5. Emi, M., Fujiwara, Y., Ohata, H., Tsuda, H., Hirohashi, S., Koike, M., Miyaki, M., Monden, M., and Nakamura, Y. (1993) Allelic loss at chromosome band 8p21.3−p22 is associated with progression of hepatocellular carcinoma, *Genes, Chromosomes Cancer 7*, 152−157.
6. van der Bosch, K., Becker, I., Savelyeva, L., Bruderlein, S., Schlag, P., and Schwab, M. (1992) Deletions in the short arm of chromosome 8 are present in up to 90% of human colorectal cancer cell lines, *Genes, Chromosomes Cancer 5*, 91−95.

7. Starcevic, D., Dalal, S., and Sweasy, J. B. (2004) Is there a link between DNA polymerase β and cancer, *Cell Cycle 3*.
8. Han, L. P., Qiao, Y. H., Dong, Z. M., Shi, H. R., Zhao, G. Q., and Liu, D. (2003) Study on DNA polymerase β gene mutation in human cervical cancer, *Zhonghua Fu Chan Ke Za Zhi 38*, 618−620.
9. Dong, Z., Zhao, G., Zhao, Q., Yang, H., Xue, L., Tan, X., and Zheng, N. (2002) A study of DNA polymerase β mutation in human esophageal cancer, *Zhonghua Yi Xue Za Zhi 82*, 899−902.
10. Dobashi, Y., Shuin, T., Tsuruga, H., Uemura, H., Torigoe, S., and Kubota, Y. (1994) DNA polymerase β gene mutation in human prostate cancer, *Cancer Res. 54*, 2827−2829.
11. Matsuzaki, J., Dobashi, Y., Miyamoto, H., Ikeda, I., Fujinami, K., Shuin, T., and Kubota, Y. (1996) DNA polymerase β gene mutations in human bladder cancer, *Mol Carcinog. 15*, 38−43.
12. Sweasy, J. B., Dalal, S., Sun, K. W., Lai, C.-C., DiMaio, D., and Lang, T. (2005) Expression of DNA polymerase β mutants in mouse cells results in cellular transformation, *Proc. Natl. Acad. Sci. USA 102*, 14350−14355.
13. Lang, T., Maitra, M., Starcevic, D., Li, S. X., and Sweasy, J. B. (2004) A DNA polymerase β mutant from colon cancer cells induces mutations, *Proc. Natl. Acad. Sci. U.S.A. 101*, 6074−6079.
14. Li, S. X., Vaccaro, J. A., and Sweasy, J. B. (1999) Involvement of phenylalanine 272 of DNA polymerase β in discriminating between correct and incorrect deoxynucleoside triphosphates, *Biochemistry 38*, 4800−4808.
15. Shah, A. M., Conn, D. A., Li, S. X., Capaldi, A., Jager, J., and Sweasy, J. B. (2001) A DNA polymerase β mutator mutant with reduced nucleotide discrimination and increased protein stability, *Biochemistry 40*, 11372−11381.
16. Shah, A. M., Li, S. X., Anderson, K. S., and Sweasy, J. B. (2001) Y265H mutator mutant of DNA polymerase β. Proper teometric alignment is critical for fidelity, *J. Biol. Chem. 276*, 10824−10831.
17. Shah, A. M., Maitra, M., and Sweasy, J. B. (2003) Variants of DNA polymerase β extend mispaired DNA due to increased affinity for nucleotide substrate, *Biochemistry 42*, 10709−10717.
18. Dalal, S., Kosa, J. L., and Sweasy, J. B. (2004) The D246V mutant of DNA polymerase β misincorporates nucleotides: Evidence for a role for the flexible loop in DNA positioning within the active site, *J. Biol. Chem. 279*, 577−584.
19. Eckert, K. A., Hile, S. E., and Vargo, P. L. (1997) Development and use of an *in vitro* HSV-tk forward mutation assay to study eukaryotic DNA polymerase processing of DNA alkyl lesions, *Nucleic Acids Res. 25*, 1450−1457.
20. Eckert, K. A., Mowery, A., and Hile, S. E. (2002) Misalignment-mediated DNA polymerase β mutations: Comparison of microsatellite and frame-shift error rates using a forward mutation assay, *Biochemistry 41*, 10490−10498.
21. Vande Berg, B. J., Beard, W. A., and Wilson, S. H. (2001) DNA structure and aspartate 276 influence nucleotide binding to human DNA polymerase β. Implication for the identity of the rate-limiting conformational change, *J. Biol. Chem. 276*, 3408−3416.
22. Washington, S. L., Yoon, M. S., Chagovetz, A. M., Li, S. X., Clairmont, C. A., Preston, B. D., Eckert, K. A., and Sweasy, J. B. (1997) A genetic system to identify DNA polymerase β mutator mutants, *Proc. Natl. Acad. Sci. U.S.A. 94*, 1321−1326.
23. Starcevic, D., Dalal, S., Jaeger, J., and Sweasy, J. B. (2005) The hydrophobic hinge region of rat DNA polymerase β is critical for substrate binding pocket geometry, *J. Biol. Chem. 280*, 28388−28393.
24. Starcevic, D., Dalal, S., and Sweasy, J. B. (2005) Hinge residue Ile260 of DNA polymerase β is important for enzyme activity and fidelity, *Biochemistry 44*, 3775−3784.
25. Beard, W. A., Shock, D. D., and Wilson, S. H. (2004) Influence of DNA structure on DNA polymerase β active site function: Extension of mutagenic DNA intermediates, *J. Biol. Chem.*
26. Joyce, C. M., and Steitz, T. A. (1994) Function and structure relationships in DNA polymerases, *Annu. Rev. Biochem. 63*, 777−822.
27. Joyce, C. M., and Steitz, T. A. (1995) Polymerase structures and function: Variations on a theme? *J. Bacteriol. 177*, 6321−6329.
28. Pelletier, H., Sawaya, M. R., Wolfle, W., Wilson, S. H., and Kraut, J. (1996) Crystal structures of human DNA polymerase β complexed with DNA: Implications for catalytic mechanism, processivity, and fidelity, *Biochemistry 35*, 12742−12761.
29. Yang, L., Beard, W. A., Wilson, S. H., Broyde, S., and Schlick, T. (2002) Polymerase β simulations suggest that Arg258 rotation is a slow step rather than large subdomain motions per se, *J. Mol. Biol. 317*, 651−671.
30. Radhakrishnan, R., and Schlick, T. (2004) Orchestration of cooperative events in DNA synthesis and repair mechanism unraveled by transition path sampling of DNA polymerase β's closing, *Proc. Natl. Acad. Sci. U.S.A. 101*, 5970−5975.
31. Beard, W. A., and Wilson, S. H. (2000) Structural design of a eukaryotic DNA repair polymerase: DNA polymerase β, *Mutat. Res. 460*, 231−244.
32. Maitra, M., Gudzelak, A., Jr., Li, S. X., Matsumoto, Y., Eckert, K. A., Jager, J., and Sweasy, J. B. (2002) Threonine 79 is a hinge residue that governs the fidelity of DNA polymerase β by helping to position the DNA within the active site, *J. Biol. Chem. 277*, 35550−35560.
33. Beard, W. A., Shock, D. D., Yang, X. P., DeLauder, S. F., and Wilson, S. H. (2002) Loss of DNA polymerase β stacking interactions with templating purines, but not pyrimidines, alters catalytic efficiency and fidelity, *J. Biol. Chem. 277*, 8235−8242.
34. Coughlin, S. S., and Hall, I. J. (2002) A review of genetic polymorphisms and prostate cancer risk, *Ann. Epidemiol. 12*, 182−196.

BI051179Z